Stratification of behavioral response to transcranial current stimulation by resting-state electrophysiology

Atalanti A. Mastakouri[a], Bernhard Schölkopf[a], Moritz Grosse-Wentrup[b]

[a] *Max Planck Institute for Intelligent Systems, Empirical Inference Department, Tübingen, Germany*
[b] *Research Group Neuroinformatics, Faculty of Computer Science, University of Vienna, Austria*

Abstract

Transcranial alternating current stimulation (tACS) enables the non-invasive, focal stimulation of brain areas in desired frequencies, intensities and spatial configurations. These attributes have raised tACS to a widely used tool in cognitive neuroscience and a promising treatment in the field of motor rehabilitation. Nevertheless, considerable heterogeneity of its behavioral effects has been reported across individuals. We present a machine learning pipeline for predicting the behavioral response to 70 Hz contralateral motor cortex-tACS from Electroencephalographic resting-state activity preceding the stimulation. Specifically, we show in a cross-over study design that high-gamma (90–160 Hz) resting-state activity predicts arm-speed response to the stimulation in a concurrent reaching task. Moreover, we show in a prospective study that the behavioral effect size of stimulation significantly increases after the stratification of subjects with our prediction method. Finally, we discuss a plausible neurophysiological mechanism that links high resting-state gamma power in motor areas to stimulation response. As such, we provide a method that can reliably distinguish responders from non-responders to tACS, prior to the stimulation treatment. This contribution could eventually bring us a step closer towards translating non-invasive brain stimulation from a research tool into a safe and effective clinical treatment.

Keywords: transcranial alternating current stimulation, tACS, EEG, motor cortex, response prediction, gamma stimulation

1. Introduction

Non-invasive brain stimulation (NIBS) modulates neural activity, behavior, and brain plasticity through the non-invasive creation of forced electrical current flows inside the brain (Wagner et al., 2007; Dayan et al., 2013). There are two main categories of NIBS: Transcranial Magnetic Stimulation (TMS), which uses external magnetic fields to force the creation of electrical potentials in the cortex that depolarize neurons and trigger action potentials (Lazzaro et al., 2004), and Transcranial Electrical Stimulation (TES) (Bestmann and Walsh, 2017), which applies weak electrical direct (tDCS) or alternating (tACS) currents on the scalp (Nitsche and Paulus, 2000). In contrast to TMS, only a fraction of this current enters the brain and causes a membrane potential change of the affected neurons, which is sufficiently strong to change their probability of generating action potentials (Antal and Herrmann., 2016).

Although the neural mechanisms of NIBS are not yet fully understood (Vosskuhl et al., 2018), NIBS applications spread in research and treatment. Applications of NIBS can be divided into three main categories: studies that probe neurophysiology (e.g., how neural oscillations are causally related) (Shafi et al., 2012; Polania et al., 2012b; Filmer et al., 2014; Sehm et al., 2012; Keeser et al., 2011; Hampson and Hoffman, 2010; Anand and Hotson, 2002), studies that investigate how brain activity gives rise to behavior and cognition (Polania et al., 2018; Vosskuhl et al., 2018; Pogosyan et al., 2009; Joundi et al., 2012; Neuling et al., 2012; Cecere et al., 2015; Lustenberger et al., 2015; Vosskuhl et al., 2015; Polania et al., 2012a; Santarnecchi et al., 2013; Sela et al., 2012), and studies that employ NIBS for rehabilitation (Schulz et al., 2013; Tortella et al., 2014; Fregni et al., 2005; Palm et al., 2014; Veniero et al., 2016).

In all three categories, NIBS studies report substantial variations in stimulation response across individual subjects, including up to 55% of non-responders (Lopez-Alonso et al., 2014; Strube et al., 2015). While non-responders decrease the statistical power of NIBS studies, this sub-group is unproblematic from an

ethical point of view. Given the reported variances in effect sizes, however, it is not unreasonable to assume that there also exist subjects with negative stimulation responses (Hashemirad et al., 2016; Moliadze et al., 2010; Triccas et al., 2016; Lopez-Alonso et al., 2014; Strube et al., 2015). Subjects with negative stimulation responses would be highly problematic from an ethical point of view, because their existence would imply that NIBS studies may violate the principle of doing no harm. This ethical concern is particularly relevant in clinical settings, where NIBS is used to cause long-term (and possibly permanent) changes (Di Pino et al., 2014; Cirillo et al., 2017). Accordingly, ethical use of NIBS demands that, first, NIBS studies consider potential negative stimulation effects in individual subjects, and, second, if such effects exist, implement a procedure that reliably identifies negative responders before the stimulation treatment.

While there is a large body of literature on adverse side-effects (Kadosh et al., 2012; Davis and Koningsbruggen, 2013; Matsumoto and Ugawa, 2017), NIBS studies typically only consider inter-subject variability in terms of positive- and non-responders, bypassing the potential ethical challenges posed by negative responders. This reservation is arguably a result of the limited understanding of the causes of inter-subject variability in NIBS. Hypothesized explanations for inter-subject variability include non-apparent variations in experimental setups (Stecher et al., 2017; Vosskuhl et al., 2018; Buch et al., 2017), individual differences in brain anatomy (Buch et al., 2017; Datta, 2012; Parazzini et al., 2015), and brain-state dependent susceptibility to NIBS (Silvanto et al., 2008; Lopez-Alonso et al., 2014; Strube et al., 2015; Wiethoff et al., 2014). Factors that have been studied empirically include priming (Ragert et al., 2009; Todd et al., 2009), prior activity (Rosenkranz et al., 2007; Iezzi et al., 2008), age (Moliadze et al., 2015; Fujiyama et al., 2014), attention (Kiers et al., 1993), sex (Pitcher et al., 2004), pharmacological influences(Ziemann et al., 2008; Grundey et al., 2012; Nitsche et al., 2004), genetic variations (Li Voti et al., 2011; Mori et al., 2011), and the time of day (Lopez-Alonso et al., 2014). There is presently no set of factors known, however, that enables a reliable identification of subjects,

who do not respond to or may even be harmed by NIBS, before the stimulation treatment (Ridding and Ziemann, 2010).

In this article, we demonstrate that inter-subject variability, as measured by the effect of γ-range (70 Hz) tACS over contralateral motor cortex on movement speed during a three-dimensional reaching task, encompasses subjects with positive- as well with negative behavioral effects that are sufficiently strong to reach statistical significance on the single-subject level. This result establishes that negative stimulation response is a serious concern for the ethical use of NIBS. We then proceed to show that electrophysiological signatures of resting-state brain activity can be used to predict individual subjects' stimulation response with high accuracy. Specifically, we present a machine learning pipeline that takes Electroencephalographic (EEG) resting-state recordings of individual subjects as input, and outputs their predicted stimulation response. We apply this pipeline to learn a stimulation response predictor for the present motor performance study, and demonstrate in a prospective study that the stimulation response predictor successfully stratifies subjects into a responder and a non-responder group with statistically significant differences in stimulation effects. In particular, our stimulation response predictor correctly identifies 16 out of 16 subjects who do not respond positively to the stimulation treatment. We then show that successful stimulation response prediction is contingent on resting-state brain signatures recorded directly before NIBS. This finding supports the interpretation that stimulation response is a state and not a trait, i.e., subjects' susceptibility to brain stimulation may vary over time.

By providing a principled approach to identify subjects, who do not benefit from or may even be harmed by NIBS, before the stimulation treatment, our work constitutes an essential step towards an effective and ethical application of NIBS in clinical settings. Concurrently, our prediction pipeline can be employed to increase the statistical power of NIBS studies by excluding non-responders a priori. Because our results indicate that subjects' susceptibility to NIBS is a state and not a trait, administering stimulation treatments only when subjects are in a suitable state of mind may further enlarge the range of subjects who

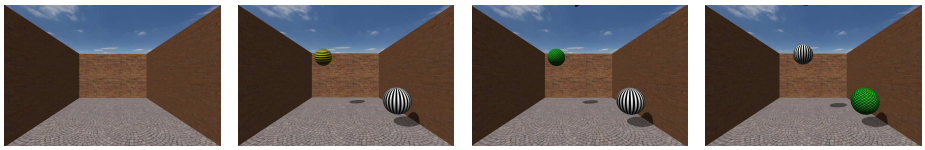

Figure 1: Phases of a trial: a) Subjects wait for the next target. b) A yellow target appears at a random location. Subjects wait for the go-cue, with their current hand position indicated by a white ball. c) A change of target color to green instructs subjects to initiate the reaching movement. d) Subjects have to move their hand back to the starting position, indicated by the green ball.

benefit from NIBS.

Adhering to best practices in open science, all experimental data and code will become publicly available upon publication. During the review process, please request code and data through the editorial staff.

The study conformed to the Declaration of Helsinki, and the experimental procedures involving human subjects described in this paper were approved by the Ethics Committee of the Medical Faculty of the Eberhard Karls University of Tübingen. Informed consent was obtained by all participants, prior to their participation to the study.

2. Material and methods

2.1. Experimental paradigm and data

Each participant attended two sessions, subsequently termed days, separated by a one day break. On each of the two days, participants were seated on a chair in the middle of four infrared motion tracking cameras (Phase Space, San Leandro, California, USA), facing a visual feedback screen (35″) at a distance of 1.5 meters, while wearing a specially designed glove with three LEDs on its top for real-time tracking of their arm location. The position of the arm was depicted on the screen in real time as a 3D sphere (cf. Figure 1).

The experimental paradigm was a 3D-reaching task. In each trial, a target sphere appeared in a simulated 3D space at a random location. The subjects'

goal was to reach the target with their right wrist by moving their arm. Each trial started with a baseline of 5 s, followed by 2.5–4 s during which the target appeared on the screen as a yellow sphere. During this period, subjects had been told to plan but not yet initiate their movement. After the target sphere changed to green, subjects had 10 s to move their arm to reach the target. After a successful reach, a score screen, indicating the movement's quality, appeared for 2 s. This score was computed as an inverse mapping of their movement's normalized averaged rectified jerk score (NARJ) to a scale from 0 to 100 (Cozens and Bhakta, 2003; Meyer et al., 2014). In the last phase of each trial, the sphere appeared at the original starting position of the subjects' wrist. The trial completed when subjects returned their wrist to the original starting position. If the reach was not completed within 10 s, or if the subject moved before the sphere turned green, the trial was excluded from further analysis.

Session 1

During the first day, only electroencephalographic (EEG) (124 active electrodes at 500 Hz sampling rate, BrainAmp DC, Brain Products, Gilching, Germany) and motion tracking (sampling rate of 960 Hz) data were recorded in parallel to the reaching task. The recording session consisted of three blocks of 50 trials each (cf. Figure 2). Before and after each block, 5 min of resting-state EEG were recorded, during which subjects were asked to relax without moving, focus their eyes on a cross on the screen, and keep their arm in a comfortable position on top of their leg.

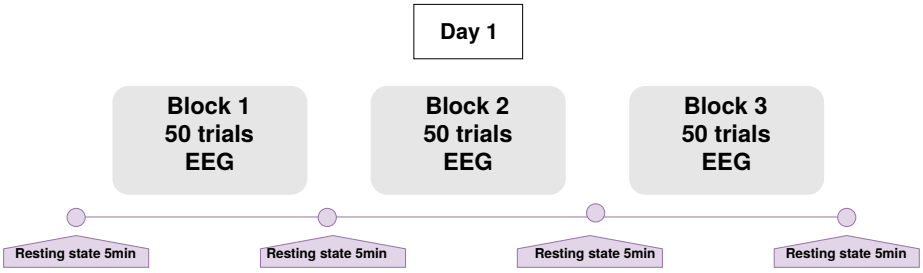

Figure 2: Experimental setup for the first recording session (no stimulation).

Session 2

The second recording day was a cross-over randomized stimulation session. This session consisted of three blocks of reaching trials of 15 min each (cf. Figure 3). During the first block, EEG and motion tracking data were recorded but subjects were not yet stimulated. During the second and third block real- and sham high-definition (HD) transcranial alternating current stimulation (tACS) was applied, respectively, in a randomized order that was not revealed to the subject. A break of 20 min was introduced between the second and the third block, during which the subject was asked to stay seated and relaxed, to avoid carry-over effects. At the end of the session, the participant completed a questionnaire to evaluate the sensation of the stimulation and potential side effects. Before and after each block, a 5 min resting-state EEG was recorded, during which subjects were asked to relax without moving, focus their eyes on a cross on the screen, and keep their arm in a comfortable position on top of their leg.

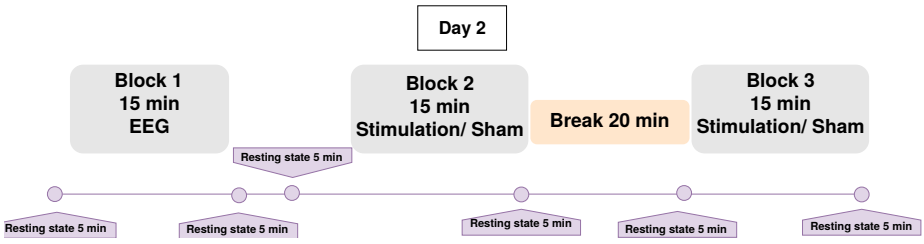

Figure 3: Experimental setup for the second recording session (with stimulation).

Stimulation setup

We employed a 4×1 HD-tACS setup (DC Stimulator Plus, neuroConn GmbH, Ilmenau, Germany) to increase spatial focality relative to the more commonly used two-electrode setup (Dmochowski et al., 2011). The equalizer extension box of the DC Stimulator Plus was used to extend the two ordinary square sponge electrodes into a 4×1 set of round rubber electrodes of 20 mm diameter (3 cm^2), with one anode in the center and four cathodes in a square at a distance of 7.5 cm from the central anode. The anode was placed over channel C3 (left primary motor cortex - M1) and the four cathodes over Cz, F3, T7, and

P3 (Villamar et al., 2013). Real stimulation was delivered at 70 Hz and 1 mA peak-to-peak amplitude, while sham stimulation was delivered at 85 Hz and 1 uA peak-to-peak amplitude.

Subjects

Twenty healthy, right-handed subjects participated in the first part of this study. One subject did not attend the second day of recordings and was excluded from further analyses. The remaining 19 subjects (nine female) had an average age of 28.37 years with a standard deviation of 8.57 years.

2.2. Analysis of behavioral data

We quantified the behavioral effect size of γ-tACS over contralateral M1 by the difference between the average reaching speed during the real- and the sham-stimulation block, because γ-tACS over motor cortex has been reported to influence movement velocity (Joundi et al., 2012; Lopez-Alonso et al., 2014; Muthukumaraswamy, 2010).. To compute the effect sizes on the level of individual subjects, we first computed, for every trial and subject, the trial-averaged reaching speed. This was done by, first, identifying the part of each trial which corresponded to the the subject's movement, i.e., from the "Go" phase until the reaching of the target. We then extracted the x, y and z coordinates from the frames of the camera and calculated the mean velocity as the amplitude of the discrete positional derivative (Meyer et al., 2014). For each subject, we computed the block-averaged reaching velocities by averaging the trial-averaged velocities within the real- and the sham-stimulation block. If a trial-averaged velocity deviated from the block-averaged velocity by more than three standard deviations the trial was rejected as an outlier. Finally, we computed the difference between the block-averaged velocities of the real- and the sham-stimulation blocks and normalized the difference by the standard deviation of each subject's sham-stimulation block to obtain the subject-level behavioral effect sizes. To compute the group-level behavioral effect size, we averaged the subject-level effect sizes and normalized by their standard deviation.

To test for a statistically significant behavioral stimulation effect on the level of individual subjects, we performed, for each subject, a two-sided, t-test on the trial-averaged arm velocities of the real- and the sham-stimulation block. We built the null-distribution by randomly permuting the assignment of trials to the real- and sham-stimulation block 10.000 times. After every permutation, we re-computed the subject's average speed difference between the real- and the sham-block. We calculated the p-value as the frequency at which samples from the null-distribution exceeded the original absolute average speed difference between the real- and the sham-block. Subjects with $p < 0.05$ and larger average speed during the real- compared to sham-block were subsequently termed *responders*. The remaining subjects were termed *non-responders*.

To test for a statistically significant behavioral stimulation effect on the group-level, we performed a two-sided, paired t-test on the single-subject effect sizes. We built the null-distribution by randomly flipping every subjectâĂŹs block-average velocities between the real- and sham-blocks 10.000 times. After random permutation, we re-computed the group-level behavioral effect size as described above. We calculated the p-value as the frequency at which samples from the null-distribution exceeded the original absolute group-level effect size.

2.3. Analysis of EEG data

We first cleaned each subject's EEG data from non-cortical artifacts by Independent Component Analysis (ICA), and then computed resting-state band-power in canonical EEG frequency bands.

For each subject and session, we concatenated the raw data of all resting-state recordings, high-pass filtered the data with a Butterworth filter at 3 Hz, and re-referenced the data to common-average reference. We then used the SOBI algorithm (Belouchrani et al., 1993) to extract 64 independent components (ICs). We manually inspected the topography of every IC, and discarded those ICs that did not show a cortical topography (McMenamin et al., 2010). The remaining cortical ICs (ranging between four and 12 across subjects) were re-projected to the scalp level, and the individual resting-state recordings were

reconstructed. For each subject, resting-state, and electrode, we normalized the data by z-scoring.

For every subject, resting-state, and electrode, we then computed log-bandpower in eight canonical EEG frequency bands: δ (1–4 Hz), θ (4–8 Hz), α (8–12 Hz), β (12–25 Hz), γ_1 (25 –45 Hz), γ_2 (45 –65 Hz), γ_3 (65 –90 Hz), and γ_4 (90–160 Hz). This was done by windowing the data with a Hamming window, computing the Discrete Fourier Transform, taking the average of the absolute values of all frequency components within each of the eight frequency bands, and finally taking the natural logarithm.

2.4. Training of the stimulation response predictor

We trained a linear discriminant analysis (LDA) classifier to predict subjects' category (*responder* vs. *non-responders*) from their resting-state EEG. Due to the small sample size, we selected two EEG channels over left- (CCP3h) and right motor cortex (CCP4h) and one channel over parietal cortex (Pz) as input to the classifier (channel C3 directly over left motor cortex was blocked by the stimulation electrodes, hence for symmetry we did not use C4 as well). For each of the eight frequency bands (cf. Section 2.3) and the three resting-state recordings on the stimulation day, we evaluated the prediction accuracy of the classifier by leave-one-subject-out cross-validation. We tested the statistical significance of each of the 24 settings (eight frequency bands times three resting-states) by a permutation test with 1000 permutations. To build the null-distribution, we randomly permuted the labels on the training set of each cross-validation fold, retrained the classifier, and classified the subject in the test set. We calculated the p-value as the frequency at which samples from the null-distribution exceeded the original prediction accuracy. We then selected the best-performing combination of frequency-band and resting-state to train the final stimulation response predictor (SRP) on all 19 subjects.

2.5. Validation of the stimulation response predictor

To validate the SRP, we recruited 22 new subjects (eleven female, average age of 26.81 years with a standard deviation of 6.32 years). We employed the

same EEG processing pipeline as for the first group of subjects (cf. Section 2.3), except that we used the EEG data of the first session (recorded on day one) to compute the ICA. To clean the EEG of the stimulation session (recorded on day two) from non-cortical artifacts, we applied the spatial filters derived on day one to the EEG data of day two, and reprojected only those ICs that corresponded to cortical sources on day one. In this way, we minimized the probability that any manual selection of ICs on day two could have confounded the predictions of the SRP. We then applied the trained SRP, as described in Section 2.4, to the first resting-state recording of every subject in the validation group, and compared the predicted categories with those derived from the behavioral analysis described in Section 2.2 (the categorization of subjects in the validation group into *responders* and *non-responders* is shown in Table .2 in the supplementary material).

To test for a statistically significant difference in the behavioral stimulation effect between the predicted responder and non-responder group, we employed a one-sided permutation-based t-test: We randomly permuted the predicted assignments of subjects to the responders- and non-responders group 10.000 times. After every permutation, we recomputed the group-level effect size within each group (responders vs. non-responders) as described in Section 2.2, and calculated the p-value as the frequency at which the permuted difference in effect sizes exceeded the original one.

2.6. Statistical power analysis

Assuming normally distributed measurements and an effect size ρ, the number of subjects required in a two-sided t-test to achieve a type I and type II error of α and β, respectively, is given by (Hickey et al., 2018)

$$N = \left(\frac{Z_{1-\alpha/2} + Z_{1-\beta}}{\rho} \right)^2, \tag{1}$$

where $Z_{(.)}$ refers to the cumulative standard normal distribution. Solving for β, we obtain

$$\beta = \frac{1}{2\pi} \int_{-\infty}^{\rho\sqrt{N} - Z_{1-\alpha/2}} e^{-t^2/2} dt \tag{2}$$

for the type II error. Plugging in the estimates of the group-level effect sizes on the validation group of $\rho_{\text{pre}} = 0.23$ and $\rho_{\text{post}} = 2.46$ before and after stratification, respectively, and assuming that these effect-size values as well as the stratification ratio of 82% (of subjects being rejected by the prediction pipeline as non-responders) observed in the validation group are accurate estimates of the population-level values, we obtain the statistical power as a function of the number of subjects shown in Figure .9 in the supplementary material. The statistical power after stratification exceeds the power before stratification for all N, with a maximal gain in power of 0.84 (582% increase of the power) for $N = 16$ subjects.

2.7. Association of stimulation response with external factors

We tested the stimulation response of individual subjects (*responders* vs. *non-responders*, cf. Section 2.2) for associations with four external factors: gender, order of the sham- and real-stimulation block, block of the strongest reported sensation of stimulation, and baseline motor performance during the first session. For all analyses, we pooled all 41 subjects from the training- and the validation group.

To test for an association of the stimulation response with gender (female, male) and order of the stimulation block, respectively, we used Fisher's exact test. To test for an association of the stimulation response with the block of the strongest sensory sensation, we employed a chi-squared test. Finally, to test for an association between the average reaching speed during the first session (on day one) with subsequent stimulation response in the second session (on day two), we performed an ANOVA for the average movement speed across all three blocks on day one. For all tests, we chose a significance level of $\alpha = 0.05$.

3. Results

3.1. Positive- and negative stimulation effects in tACS

We assessed inter-subject variability of the behavioral response to tACS in a motor performance study with a cross-over design. Twenty healthy subjects

performed 15-minute blocks of 3D reaching movements with their right hand to targets appearing at random locations in a 2D visual feedback setup (Figure 1).

Figure 4 shows the histogram and estimated probability density function (Gaussian kernel density estimate with a kernel width of 0.5 (Turlach, 1999; Scott, 1992)) of effect sizes across subjects. While the group-level effect size of 0.33 is not statistically significant ($p = 0.1018$, subject-level permutation-based paired t-test, cf. Section 2.2), we found a substantial variation in the effect sizes of individual subjects, ranging from -1.12 to 1.51 with a standard deviation of 0.72. Statistical tests for significant effect sizes at the individual subject level revealed seven subjects with a statistically significant *positive* and four subjects with a statistically significant *negative* effect size (at significance level $\alpha = 0.05$, two-sided trial-level permutation-based t-test). The remaining eight subjects did not show a statistically significant effect at the individual subject level (individual p-values are shown in Table .1 in the supplementary material). These results establish that γ-tACS can have positive- as well as negative behavioral effects on motor performance, which poses an ethical challenge to tACS studies. In the following section, we demonstrate how to address this challenge by predicting individual subjects' stimulation response from their resting-state configuration of brain rhythms.

3.2. Resting-state EEG predicts tACS stimulation response

Before and after each block, we recorded a high-density resting-state electroencephalogram (EEG), manually cleaned the data from non-cortical artifacts, and computed subject-specific log-bandpower estimates for all channels in canonical EEG frequency bands ranging from 1–160 Hz (the EEG analysis is described in detail in Section 2.3). We then separated subjects into those with a statistically significant positive stimulation response, subsequently called the *responders*, and the remaining subjects, subsequently termed the *non-responders* (cf. Section 2.2). The group-average topography of power in the γ-range (90–160 Hz), recorded prior to the first (real- or sham-) stimulation block, revealed strong resting-state γ-power over contralateral motor cortex in the *responders*

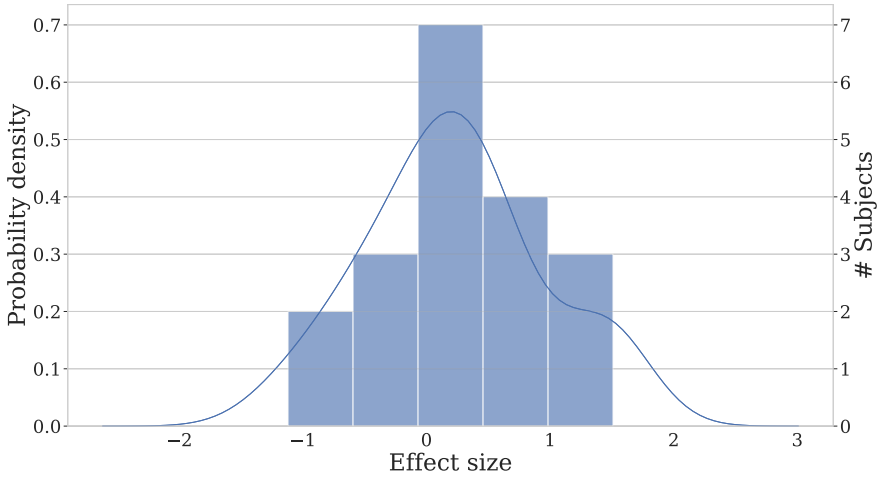

Figure 4: Histogram and estimated probability density function of stimulation response.

but not in the *non-responders* (Figure 5). This result suggests that only those subjects, who already had strong γ-power over contralateral motor cortex before the start of the stimulation, showed a subsequent positive behavioral response to contralateral γ-tACS. To systematically evaluate the predictive value of resting-state brain rhythms for stimulation response, we trained a machine learning algorithm to predict individual subjects' responses to γ-tACS from their resting-state brain rhythms. Specifically, we selected three EEG channels over left motor, right motor and central parietal cortex, computed log-bandpower during the resting-state recorded prior to the first stimulation block in canonical frequency bands, and then employed a leave-one-subject-out cross-validation procedure to assess the ability of a linear discriminant classifier (LDA) to predict each subject's group (responder vs. non-responder). The details of the prediction pipeline are described in Section 2.4. We found the prediction accuracy to increase with frequency, peaking at 89.47% in the band from 90–160 Hz ($p < 0.001$, permutation test, cf. Section 2.4 for details). Prediction accuracies and p-values for all frequency bands are shown in Figure .7 in the supplementary material. To test the robustness of the prediction pipeline, we repeated the

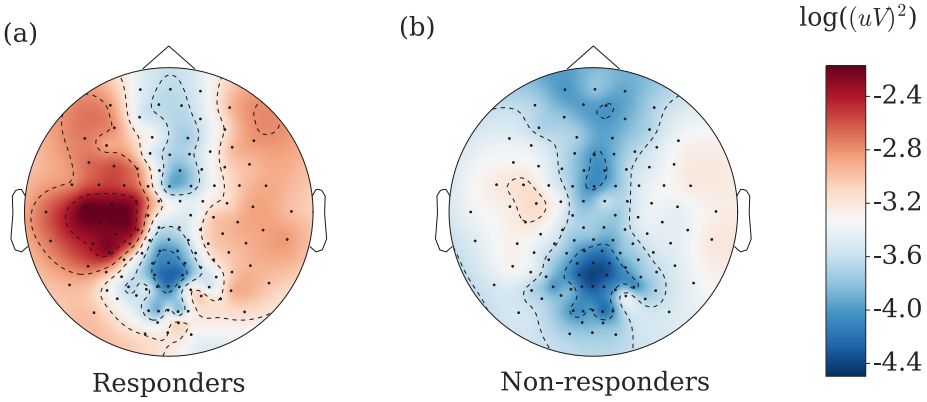

Figure 5: Group-averages for responders (a) and non-responders (b) of high γ (90–160 Hz) log-bandpower during the resting state recorded at the end of the first block of the second session (prior to stimulation blocks).

machine learning procedure for all three resting-state recordings preceding the first stimulation block. We found that all resting state recordings enabled above chance level prediction in the 90–160 Hz band. Prediction accuracies of the remaining bands varied across the different resting states. These results establish that distribution of γ-power across motor areas, as shown in Figure 5, is an accurate predictor of subjects' behavioral response to γ-tACS over contralateral motor cortex.

3.3. Subject stratification by resting-state EEG enhances effect sizes

To evaluate the practical utility of the response stratification pipeline described in the previous section, we performed an additional validation study with 22 new participants. Based on the results described in the previous section, we chose the classifier trained on the resting-state recorded after the first block in the 90–160 Hz frequency band for the validation study. This classifier was trained on the first group of subjects and then used out-of-the-box to predict the stimulation response for each subject in the validation group from a resting-state EEG recorded prior to the first block of trials (see Section 2.5 for details).

In the validation group, we observed a group-level behavioral effect size of 0.12 ($p = 0.2847$, subject-level permutation paired t-test), with subject-level effect sizes ranging from -0.94 to 1.19 (see Figure .8 in the supplementary material). The EEG-based stratification of subjects resulted in group-level effect sizes of 2.46 and -0.17 for the predicted responders and non-responders, respectively, a statistically ($p = 0.0048$, one-sided permutation-based t-test) and practically highly significant difference. In particular, all four subjects with a statistically significant negative- and all 12 subjects with no statistically significant stimulation response were correctly assigned to the group of non-responders. Further, only two subjects with a statistically significant positive stimulation response were mis-classified as non-responders. These behavioral results are summarized in Figure 6. The group-averaged topographies of log-bandpower in the γ-range of the predicted responders and non-responders, which closely resemble those observed in the training group shown in Figure 5, are displayed in Figure .10 in the supplementary material.

Based on our results, we estimate that our stratification pipeline can enhance the statistical power of brain stimulation studies by up to 582% (see Figure .9 in the supplementary material and Section 2.6). For instance, a statistical power of 95% at a type II error of 5% would require 12 and 240 subjects with and without our stratification pipeline, respectively.

3.4. Stimulation response is contingent on brain state

In a next step, we employed the validated prediction pipeline to test whether stimulation response is a state or a trait, i.e., whether subjects' response to γ-tACS changes or remains invariant over time. To do so, we pooled all 41 subjects, trained our prediction pipeline on the γ-power (90–160 Hz) of each of the four EEG resting states of their first session, i.e., two days before the stimulation session, and predicted the stimulation response in the second session with leave-one-subject-out cross-validation (all other settings were identical to those described in Sections 2.3 and 2.4). A statistically significant prediction accuracy in this setting would imply that the configuration of subjects' brain

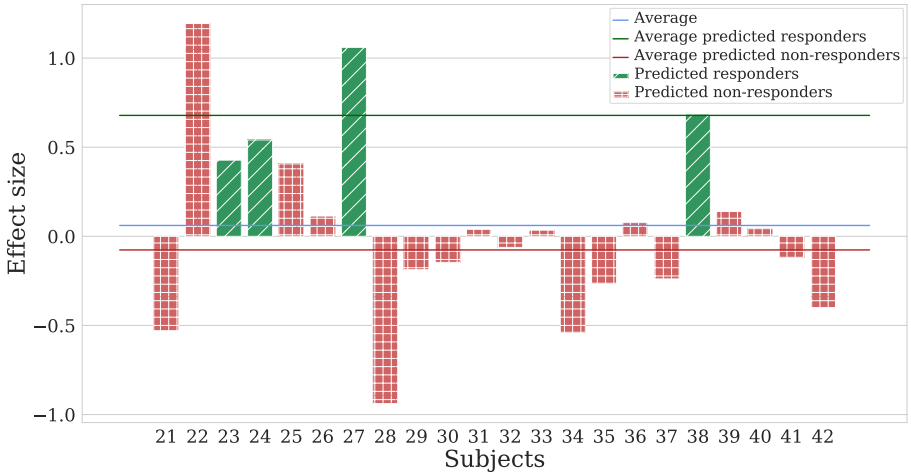

Figure 6: Individual effect-sizes and predicted stimulation responses in the validation group.

rhythms is also predictive for their stimulation response two days later. We did not, however, find any evidence in favor of this conclusion. Instead, training on brain activity of the first recording session resulted in statistically non-significant prediction accuracies between 62.5% and 68.3% (p-values of 0.23, 0.24, 0.27 and 0.73 for the four resting states of day one). This observation implies that stimulation response is contingent on subjects' brain-state directly prior to the stimulation, i.e., subjects' stimulation response is a state and not a trait.

Applying the original stimulus-response predictor, as described in Section 2.5, to the resting-state recordings of the first day, we estimate that out of the 28 subjects, who did not respond positively to the stimulation on day two, five subjects would have responded positively on day one (prediction results for individual subjects are shown in Table .3 in the supplementary material). As such, the percentage of subjects, who can benefit from tACS, may increase if they are stimulated at the right time.

4. Discussion

Our results demonstrate, first, that resting-state signatures of human brain rhythms, recorded prior to NIBS, can distinguish responders from non-responders with high accuracy, and, second, that such a stratification enhances behavioral effect sizes in empirical studies. The former contribution is essential for a safe and ethical application of NIBS in research and treatment. Because NIBS can have behavioral effects of opposite polarity relative to the intended stimulation effect in individual subjects (cf. Section 3.1), a reliable exclusion criterion for subjects with a negative stimulation response ensures that no subjects are harmed. This issue is of particular relevance in clinical settings, where NIBS is employed to cause long-term and, possibly, permanent changes. Our second finding, on the other hand, may be used to increase the statistical power of NIBS studies in research as well as in clinical settings. By excluding non-responders a-priori, we estimate that a gain of up to 582% in statistical power can be obtained.

We found strong resting-state γ-power over contralateral motor cortex to be indicative of a positive stimulation response to tACS in the same area and frequency range. As we outline in the following, this finding is in line with our current understanding of the neurophysiological effects of γ-tACS and the role of γ-power in fronto-parietal networks for motor performance (Gonzalez Andino et al., 2005). Resting-state γ-power in primary motor cortex positively correlates with γ-aminobutyric acid (GABA) levels (Chen et al., 2014; Muthukumaraswamy et al., 2009; Bartos et al., 2007; Wang and Buzsáki, 1996; Brunel and Wang, 2003). Because γ-tACS over motor cortex decreases GABA (Nowak et al., 2017), and decreases in motor cortex GABA levels correlate with increased motor performance (Stagg et al., 2011), high resting-state γ-power may signal a brain state in which motor performance can be improved through tACS-induced reduction of GABA levels. Low resting-state γ-power, in contrast, would signal a brain state in which GABA levels are already low, thus limiting the extent of potential further reduction by γ-tACS. We note that this explanation is also

in line with our finding that stimulation response is contingent on the current brain state (cf. Section 3.4).

To further probe the state vs. trait hypothesis, we tested a range of subject traits and experimental factors, including gender, order of real-/sham-stimulation, block of strongest-reported stimulation sensation and behavioral performance on the first day of the experiment, for associations with stimulation response. None of these factors reached a statistically significant association (Fisher's exact test, Chi-squared test and ANOVA, see Section 2.7). This observation is in line with previous work on explaining individual subjects' stimulation response (cf. Section 1), and underlines the significance of subjects' current brain state for their stimulation response.

Our results further indicate that the percentage of subjects, who can benefit from NIBS, may be increased when subjects are stimulated at the right time. Concurrently, the neurophysiological interpretation of our results raises the question whether the effects of stimulation lie within the range of normal variations in behavioral performance, i.e., whether NIBS induces a beneficial state of mind that can also occur spontaneously, or whether NIBS can enhance behavioral performance beyond subjects' natural limits. Either way, a natural extension of our stimulation response prediction pipeline would be to consider multiple stimulation settings that vary in parameters such as spatial and spectral focus, paving the way for personalized NIBS.

5. Conclusions

The identification of responders and non-responders prior to the application of stimulation treatment is an important first step towards personalized brain stimulation. In our work, we show that resting-state high-gamma power prior to stimulation enables this differentiation. Specifically, we demonstrate that subjectsâĂŹ resting-state EEG predicts their motor response (arm speed) to gamma (70 Hz) transcranial alternating current stimulation (tACS) over the contralateral motor cortex. We then ascertain in a prospective study with new

subjects that our prediction pipeline achieves a reliable stratification of subjects into a responder and a non-responder group.

References

Anand S, Hotson J. Transcranial magnetic stimulation: Neurophysiological applications and safety. Brain and Cognition 2002;50(3):366 –86.

Antal A, Herrmann. CS. Current and random noise stimulation: Possible mechanisms. Neural Plasticity 2016;.

Bartos M, Vida I, Jonas P. Synaptic mechanisms of synchronized gamma oscillations in inhibitory interneuron networks. Nature Reviews Neuroscience 2007;8:45.

Belouchrani A, Abed-meraim K, Cardoso JF, Moulines E. Second order blind separation of temporally correlated sources. in Proceedings of International Conference on Digital Signal Processing 1993;:346–51.

Bestmann S, Walsh V. Transcranial electrical stimulation. Current Biology 2017;27(23):R1258 –62.

Brunel N, Wang XJ. What determines the frequency of fast network oscillations with irregular neural discharges? synaptic dynamics and excitation-inhibition balance. Journal of Neurophysiology 2003;90(1):415–30.

Buch ER, Santarnecchi E, Antal A, Born J, Celnik PA, Classen J, Gerloff C, Hallett M, Hummel FC, Nitsche MA, Pascual-Leone A, Paulus WJ, Reis J, Robertson EM, Rothwell JC, Sandrini M, Schambra HM, Wassermann EM, Ziemann U, Cohen LG. Effects of tdcs on motor learning and memory formation: A consensus and critical position paper. Clinical Neurophysiology 2017;128(4):589 – 603.

Cecere R, Rees G, Romei V. Individual differences in alpha frequency drive crossmodal illusory perception. Current Biology 2015;25(2):231 –5.

Chen CMA, Stanford AD, Mao X, Abi-Dargham A, Shungu DC, Lisanby SH, Schroeder CE, Kegeles LS. Gaba level, gamma oscillation, and working memory performance in schizophrenia. NeuroImage: Clinical 2014;4:531 –9.

Cirillo G, Di Pino G, Capone F, Ranieri F, Florio L, Todisco V, Tedeschi G, Funke K, Di Lazzaro V. Neurobiological after-effects of non-invasive brain stimulation. Brain Stimulation 2017;10(1):1 – 18.

Cozens JA, Bhakta BB. Measuring movement irregularity in the upper motor neuron syndrome using normalised average rectified jerk. Journal of Electromyography and Kinesiology 2003;13(1):73–81.

Datta A. Inter-individual variation during transcranial direct current stimulation and normalization of dose using mri-derived computational models. Frontiers in Psychiatry 2012;3:91.

Davis N, Koningsbruggen M. âĂIJnon-invasiveâĂİ brain stimulation is not non-invasive. Frontiers in Systems Neuroscience 2013;7:76.

Dayan E, Censor N, Buch ER, Sandrini M, Cohen LG. Noninvasive brain stimulation: from physiology to network dynamics and back. Nature Neuroscience 2013;16:838.

Di Pino G, Pellegrino G, Assenza G, Capone F, Ferreri F, Formica D, Ranieri F, Tombini M, Ziemann U, Rothwell J, Di Lazzaro V. Modulation of brain plasticity in stroke: A novel model for neurorehabilitation. Nature reviews Neurology 2014;10:597âĂŞ–608.

Dmochowski JP, Datta A, Bikson M, Su Y, Parra LC. Optimized multi-electrode stimulation increases focality and intensity at target. Journal of Neural Engineering 2011;8:046011.

Filmer HL, Dux PE, Mattingley JB. Applications of transcranial direct current stimulation for understanding brain function. Trends in Neurosciences 2014;37(12):742 –53.

Fregni F, Simon DK, Wu A, Pascual-Leone A. Non-invasive brain stimulation for parkinson's disease: a systematic review and meta-analysis of the literature. Journal of Neurology, Neurosurgery & Psychiatry 2005;76(12):1614–23.

Fujiyama H, Hyde J, Hinder MR, Kim SJ, McCormack GH, Vickers JC, Summers JJ. Delayed plastic responses to anodal tdcs in older adults. Frontiers in Aging Neuroscience 2014;6:115.

Gonzalez Andino SL, Michel CM, Thut G, Landis T, Grave de Peralta R. Prediction of response speed by anticipatory high-frequency (gamma band) oscillations in the human brain. Human Brain Mapping 2005;24(1):50–8.

Grundey J, Thirugnanasambandam N, Kaminsky K, Drees A, Skwirba A, Lang N, Paulus W, Nitsche M. Rapid effect of nicotine intake on neuroplasticity in non-smoking humans. Frontiers in Pharmacology 2012;3:186.

Hampson M, Hoffman R. Transcranial magnetic stimulation and connectivity mapping: Tools for studying the neural bases of brain disorders. Frontiers in Systems Neuroscience 2010;4:40.

Hashemirad F, Zoghi M, Fitzgerald P, Jaberzadeh S. The effect of anodal transcranial direct current stimulation on motor sequence learning in healthy individuals: A systematic review and meta-analysis. Brain and Cognition 2016;102:1–12.

Hickey GL, Grant SW, Dunning J, Siepe M. Statistical primer: sample size and power calculations why, when and how? European Journal of Cardio-Thoracic Surgery 2018;54(1):4–9.

Iezzi E, Conte A, Suppa A, Agostino R, Dinapoli L, Scontrini A, Berardelli A. Phasic voluntary movements reverse the aftereffects of subsequent theta-burst stimulation in humans. Journal of Neurophysiology 2008;100(4):2070–6.

Joundi RA, Jenkinson N, Brittain JS, Aziz TZ, Brown P. Driving oscillatory activity in the human cortex enhances motor performance. Current Biology 2012;22(5):403–7.

Kadosh RC, Levy N, O'Shea J, Shea N, Savulescu J. The neuroethics of non-invasive brain stimulation. Current Biology 2012;22(4):R108 –11.

Keeser D, Meindl T, Bor J, Palm U, Pogarell O, Mulert C, Brunelin J, MÃűller HJ, Reiser M, Padberg F. Prefrontal transcranial direct current stimulation changes connectivity of resting-state networks during fmri. Journal of Neuroscience 2011;31(43):15284–93.

Kiers L, Cros D, Chiappa K, Fang J. Variability of motor potentials evoked by transcranial magnetic stimulation. Electroencephalography and Clinical Neurophysiology/Evoked Potentials Section 1993;89(6):415 –23.

Lazzaro VD, Oliviero A, Pilato F, Saturno E, Dileone M, Mazzone P, Insola A, Tonali P, Rothwell J. The physiological basis of transcranial motor cortex stimulation in conscious humans. Clinical Neurophysiology 2004;115(2):255 –66.

Li Voti P, Conte A, Suppa A, Iezzi E, Bologna M, Aniello MS, Defazio G, Rothwell JC, Berardelli A. Correlation between cortical plasticity, motor learning and bdnf genotype in healthy subjects. Experimental Brain Research 2011;212(1):91–9.

Lopez-Alonso V, Cheeran B, Rio-Rodriguez D, del Olmo MF. Inter-individual variability in response to non-invasive brain stimulation paradigms. Brain Stimulation 2014;7(3):372 –80.

Lustenberger C, Boyle MR, Foulser AA, Mellin JM, Frohlich F. Functional role of frontal alpha oscillations in creativity. Cortex 2015;67:74 – 82.

Matsumoto H, Ugawa Y. Adverse events of tdcs and tacs: A review. Clinical Neurophysiology Practice 2017;2:19 – 25.

McMenamin BW, Shackman AJ, Maxwell JS, Bachhuber DR, Koppenhaver AM, Greischar LL, Davidson RJ. Validation of ica-based myogenic artifact correction for scalp and source-localized eeg. NeuroImage 2010;49(3):2416 –32.

Meyer T, Peters J, Zander T, Schölkopf B, Grosse-Wentrup M. Predicting motor learning performance from electroencephalographic data. Journal of NeuroEngineering and Rehabilitation 2014;11:24.

Moliadze V, Antal A, Paulus W. Boosting brain excitability by transcranial high frequency stimulation in the ripple range. The Journal of Physiology 2010;588(24):4891–904.

Moliadze V, Schmanke T, Andreas S, Lyzhko E, Freitag CM, Siniatchkin M. Stimulation intensities of transcranial direct current stimulation have to be adjusted in children and adolescents. Clinical Neurophysiology 2015;126(7):1392 –9.

Mori F, Ribolsi M, Kusayanagi H, Siracusano A, Mantovani V, Marasco E, Bernardi G, Centonze D. Genetic variants of the nmda receptor influence cortical excitability and plasticity in humans. Journal of Neurophysiology 2011;106(4):1637–43.

Muthukumaraswamy SD. Functional properties of human primary motor cortex gamma oscillations. Journal of Neurophysiology 2010;104(5):2873–85.

Muthukumaraswamy SD, Edden RA, Jones DK, Swettenham JB, Singh KD. Resting gaba concentration predicts peak gamma frequency and fmri amplitude in response to visual stimulation in humans. Proceedings of the National Academy of Sciences 2009;106(20):8356–61.

Neuling T, Rach S, Wagner S, Wolters C, Herrmann C. Good vibrations: Oscillatory phase shapes perception. NeuroImage 2012;63(2):771 –8.

Nitsche MA, Jaussi W, Liebetanz D, Lang N, Tergau F, Paulus W. Consolidation of human motor cortical neuroplasticity by d-cycloserine. Neuropsychopharmacology 2004;29:1573.

Nitsche MA, Paulus W. Excitability changes induced in the human motor cortex by weak transcranial direct current stimulation. The Journal of Physiology 2000;527:1469 – 7793.

Nowak M, Hinson E, van Ede F, Pogosyan A, Guerra A, Quinn A, Brown P, Stagg CJ. Driving human motor cortical oscillations leads to behaviorally relevant changes in local gabaa inhibition: A tacs-tms study. Journal of Neuroscience 2017;37(17):4481–92.

Palm U, Ayache S, Padberg F, Lefaucheur JP. Non-invasive brain stimulation therapy in multiple sclerosis: A review of tdcs, rtms and ect results. Brain Stimulation 2014;7.

Parazzini M, Fiocchi S, Liorni I, Ravazzani P. Effect of the interindividual variability on computational modeling of transcranial direct current stimulation. Computational Intelligence and Neuroscience 2015;.

Pitcher JB, Ogston KM, Miles TS. Age and sex differences in human motor cortex input output characteristics. The Journal of Physiology 2004;546(2):605–13.

Pogosyan A, Doyle Gaynor L, Eusebio A, Brown P. Boosting cortical activity at beta-band frequencies slows movement in humans. Current Biology 2009;19(19):1637 –41.

Polania R, Nitsche MA, Korman C, Batsikadze G, Paulus W. The importance of timing in segregated theta phase-coupling for cognitive performance. Current Biology 2012a;22(14):1314 –8.

Polania R, Nitsche MA, Ruff CC. Studying and modifying brain function with non-invasive brain stimulation. Nature Neuroscience 2018;21:174–87.

Polania R, Paulus W, Nitsche M. Modulating cortico-striatal and thalamo-cortical functional connectivity with transcranial direct current stimulation. Human Brain Mapping 2012b;33(10):2499–508.

Ragert P, Camus M, Vandermeeren Y, Dimyan MA, Cohen LG. Modulation of effects of intermittent theta burst stimulation applied over primary motor cortex (m1) by conditioning stimulation of the opposite m1. Journal of Neurophysiology 2009;102(2):766–73.

Ridding MC, Ziemann U. Determinants of the induction of cortical plasticity by non-invasive brain stimulation in healthy subjects. The Journal of Physiology 2010;588(13):2291–304.

Rosenkranz K, Kacar A, Rothwell JC. Differential modulation of motor cortical plasticity and excitability in early and late phases of human motor learning. Journal of Neuroscience 2007;27(44):12058–66.

Santarnecchi E, Polizzotto NR, Godone M, Giovannelli F, Feurra M, Matzen L, Rossi A, Rossi S. Frequency-dependent enhancement of fluid intelligence induced by transcranial oscillatory potentials. Current Biology 2013;23(15):1449 –53.

Schulz R, Gerloff C, Hummel FC. Non-invasive brain stimulation in neurological diseases. Neuropharmacology 2013;64:579 –87.

Scott DW. Multivariate density estimation: Theory, practice, and visualization. John Wiley and Sons 1992;.

Sehm B, SchÃďfer A, Kipping J, Margulies D, Conde V, Taubert M, Villringer A, Ragert P. Dynamic modulation of intrinsic functional connectivity by transcranial direct current stimulation. Journal of Neurophysiology 2012;108(12):3253–63.

Sela T, Kilim A, Lavidor M. Transcranial alternating current stimulation increases risk-taking behavior in the balloon analog risk task. Frontiers in Neuroscience 2012;6:22.

Shafi M, Westover M, Fox M, Pascual-Leone A. Exploration and modulation of brain network interactions with noninvasive brain stimulation in combination with neuroimaging. European Journal of Neuroscience 2012;35(6):805–25.

Silvanto J, Cattaneo Z, Battelli L, Pascual-Leone A. Baseline cortical excitability determines whether tms disrupts or facilitates behavior. Journal of Neurophysiology 2008;99(5):2725–30.

Stagg CJ, Bachtiar V, Johansen-Berg H. The role of gaba in human motor learning. Current Biology 2011;21(6):480 –4.

Stecher HI, Pollok TM, StrÃijber D, Sobotka F, Herrmann CS. Ten minutes of α-tacs and ambient illumination independently modulate eeg α-power. Frontiers in Human Neuroscience 2017;11:257.

Strube W, Bunse T, Malchow B, Hasan A. Efficacy and interindividual variability in motor-cortex plasticity following anodal tdcs and paired-associative stimulation. Neural Plasticity 2015;(530423).

Todd G, Flavel SC, Ridding MC. Priming theta-burst repetitive transcranial magnetic stimulation with low- and high-frequency stimulation. Experimental Brain Research 2009;195(2):307–15.

Tortella G, Selingardi PM, Moreno ML, Veronezi BP, Brunoni AR. Does non-invasive brain stimulation improve cognition in major depressive disorder? a systematic review. CNS Neurological Disorders - Drug Targets 2014;13:1759 –69.

Triccas LT, Burridge J, Hughes A, Pickering R, Desikan M, Rothwell J, Verheyden G. Multiple sessions of transcranial direct current stimulation and upper extremity rehabilitation in stroke: A review and meta-analysis. Clinical Neurophysiology 2016;127(1):946 –55.

Turlach B. Bandwidth selection in kernel density estimation: A review. Technical Report 1999;.

Veniero D, Stru ber D, Thut G, Herrmann C. Noninvasive brain stimulation techniques can modulate cognitive processing. Organizational Research Methods 2016;.

Villamar MF, Volz MS, Bikson M, Datta A, DaSilva AF, Fregni F. Considerations in the use of 4x1 ring high-definition transcranial direct current stimulation (hd-tdcs). Journal of Visualized Experiments 2013;77:e50309.

Vosskuhl J, Huster RJ, Herrmann CS. Increase in short-term memory capacity induced by down-regulating individual theta frequency via transcranial alternating current stimulation. Frontiers in Human Neuroscience 2015;9:257.

Vosskuhl J, StrÃijber D, Herrmann CS. Non-invasive brain stimulation: A paradigm shift in understanding brain oscillations. Frontiers in Human Neuroscience 2018;12:211.

Wagner T, Valero-Cabre A, Pascual-Leone A. Noninvasive human brain stimulation. Annual Review of Biomedical Engineering 2007;9(1):527–65.

Wang XJ, Buzsáki G. Gamma oscillation by synaptic inhibition in a hippocampal interneuronal network model. Journal of Neuroscience 1996;16(20):6402–13.

Wiethoff S, Hamada M, Rothwell JC. Variability in response to transcranial direct current stimulation of the motor cortex. Brain Stimulation 2014;7(3):468 –75.

Ziemann U, Paulus W, Nitsche MA, Pascual-Leone A, Byblow WD, Berardelli A, Siebner HR, Classen J, Cohen LG, Rothwell JC. Consensus: Motor cortex plasticity protocols. Brain Stimulation 2008;1(3):164 –82.

Appendices

Table .1: Categorization of subjects into *responders* and *non-responders*, first group of recordings. ΔVelocity > 0 refers to subjects with a higher movement speed in the real- vs. the sham-stimulation block.

Subject	p-value	ΔVelocity > 0	Category
1	0.0005	1	responder
2	0.6217	1	non-responder
3	0.0902	1	non-responder
4	0.0121	0	non-responder
5	<0.0001	1	responder
6	0.9318	1	non-responder
7	0.3979	1	non-responder
8	0.1628	1	non-responder
9	0.9220	0	non-responder
11	0.0154	0	non-responder
12	0.0251	1	responder
13	0.0384	0	non-responder
14	0.0800	0	non-responder
15	0.8484	1	non-responder
16	<0.0001	1	responder
17	<0.0001	0	non-responder
18	0.0077	1	responder
19	0.0370	1	responder
20	0.0455	1	responder

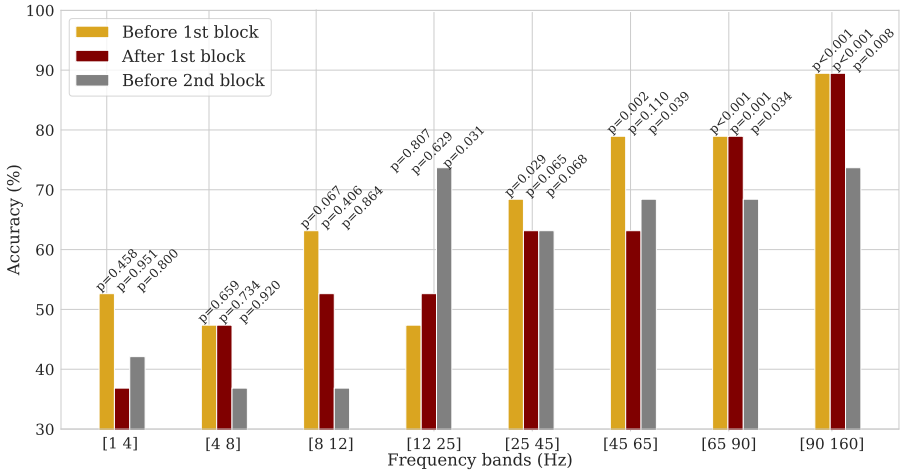

Figure .7: Leave-one-subject-out cross-validated prediction accuracy of stimulation response in the first group of subjects across canonical frequency bands and resting-states, cf. Section 2.4 for details. Stimulation day (day 2).

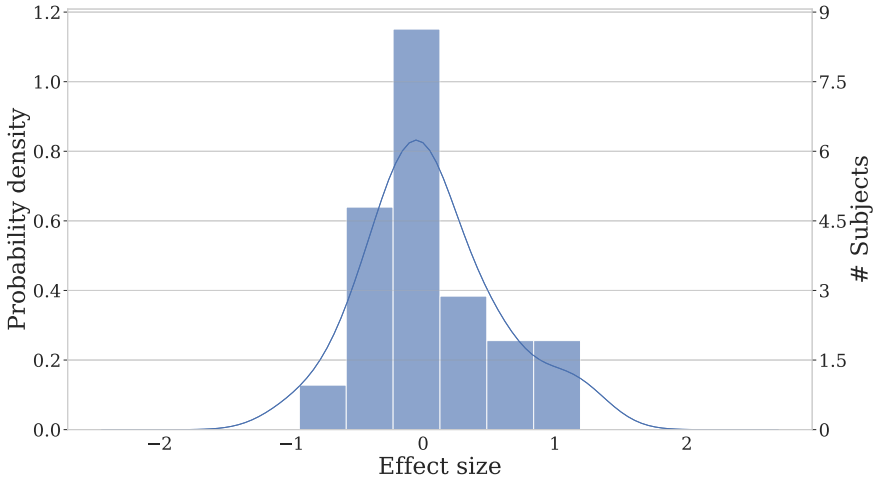

Figure .8: Histogram and estimated probability density function of stimulation response in the validation group.

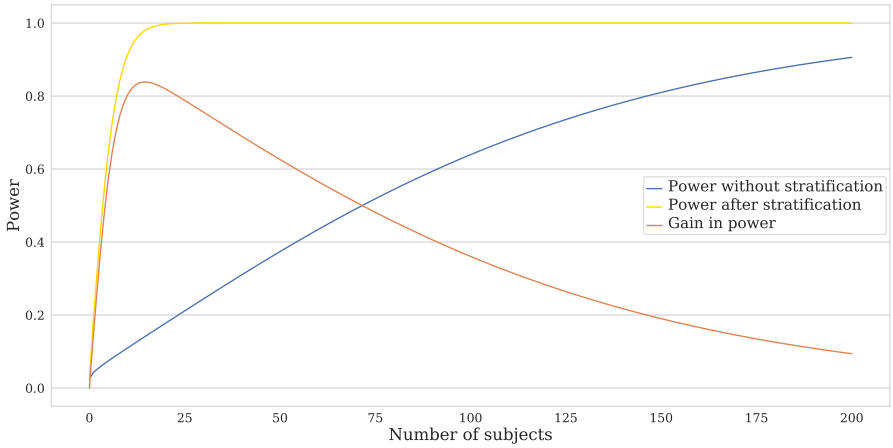

Figure .9: Statistical power as a function of the number of subjects with and without stratification by the SRP pipeline with type II error fixed at $\alpha = 0.05$.

Table .2: Categorization of subjects into *responders* and *non-responders*, second (validation) group of recordings. ΔVelocity > 0 refers to subjects with a higher movement speed in the real- vs. the sham-stimulation block.

Subject	p-value	ΔVelocity > 0	Category
21	0.0001	0	non-responder
22	0.0004	1	responder
23	0.0119	1	responder
24	0.0093	1	responder
25	0.0353	1	responder
26	0.5704	1	non-responder
27	0.0001	1	responder
28	$<$0.0001	0	non-responder
29	0.5334	0	non-responder
30	0.5449	0	non-responder
31	0.6537	1	non-responder
32	0.8046	0	non-responder
33	0.8770	1	non-responder
34	0.0055	0	non-responder
35	0.0678	0	non-responder
36	0.6119	1	non-responder
37	0.2996	0	non-responder
38	0.0048	1	responder
39	0.4444	1	non-responder
40	0.7515	1	non-responder
41	0.5464	0	non-responder
42	0.0075	0	non-responder

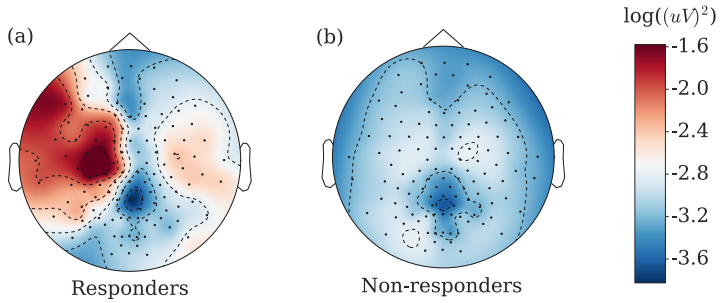

Figure .10: Group-averages for predicted responders (a) and non-responders (b) in the validation group of high γ (90–160 Hz) log-bandpower during the resting state recorded at the beginning of the stimulation day (prior to stimulation blocks).

Table .3: Subjects' predicted behavioral response from resting-state EEG data recorded on day one versus actual behavioral response measured on day two.

Subjects predicted as responders on day one	15, 18, 19, 22, 23, 24, 27, 33, 34, 36, 38, 42
Actual non-responders on day two	2, 3, 4, 6, 7, 8, 9, 11, 13, 14, 15, 17, 21, 26, 28, 29, 30, 32, 33, 34, 35, 36, 37, 39, 40, 41, 42
Intersection	15, 33, 34, 36, 42